View metadata, citation and similar papers at core.ac.uk

brought to you by CORE

provided by University of Bath Research Portal

Citation for published version:
De Oliveira, REP, Knight, JC, Taru, T & De Matos, CJS 2013, 'Temperature response of an all-solid photonic bandgap fiber for sensing applications', Applied Optics, vol. 52, no. 7, pp. 1461-1467. https://doi.org/10.1364/AO.52.001461

DOI:
10.1364/AO.52.001461

Publication date:
2013

Document Version
Publisher's PDF, also known as Version of record

Link to publication

This paper was published in Applied Optics and is made available as an electronic reprint with the permission of OSA. The paper can be found at the following URL on the OSA website: http://dx.doi.org/10.1364/AO.52.001461 . Systematic or multiple reproduction or distribution to multiple locations via electronic or other means is prohibited and is subject to penalties under law.

University of Bath

General rights
Copyright and moral rights for the publications made accessible in the public portal are retained by the authors and/or other copyright owners and it is a condition of accessing publications that users recognise and abide by the legal requirements associated with these rights.

Take down policy
If you believe that this document breaches copyright please contact us providing details, and we will remove access to the work immediately and investigate your claim.

Download date: 13. May. 2019

Temperature response of an all-solid photonic bandgap fiber for sensing applications

Rafael E. P. de Oliveira,[1,*] Jonathan C. Knight,[2] Toshiki Taru,[2] and Christiano J. S. de Matos[1]

[1]Grupo de Fotônica—Universidade Presbiteriana Mackenzie, São Paulo 01302-907, Brazil

[2]Centre for Photonics and Photonic Materials and Department of Physics, University of Bath, Bath BA2 7AY, UK

*Corresponding author: rafael.oliveira1@mackenzie.br

Received 20 November 2012; revised 4 February 2013; accepted 5 February 2013; posted 5 February 2013 (Doc. ID 180216); published 28 February 2013

The spectral shift due to temperature in the photonic bandgap (PBG) of an all-solid PBG fiber is investigated, aiming at discrete and distributed temperature sensing. A temperature rise induces a red shift in the bandgap spectra, which can be easily and precisely monitored by measuring the fiber transmission near one of the band edges. Two different situations that are potentially compatible with distributed and quasi-distributed sensing were investigated: heating a 2 m section of a longer (~10 m) fiber, and heating the whole extension of a fiber that is tens of centimeters in length and was spliced to conventional fibers on both sides. The latter setup yielded bandgap spectral shifts up to ~35 pm/°C. Aiming at discrete sensing, a short (~50 mm) fiber section was subjected to a tight bend so as to exhibit increased temperature sensitivity. Choosing the position of the bend allows for reconfiguration, on demand, of the sensor. A semi-analytical method to identify the spectral position of bandgaps was used to model the fiber transmission, as well as the bandgap shift with temperature, with consistent results. © 2013 Optical Society of America

OCIS codes: 060.2270, 060.2370, 060.5295, 120.6780.

1. Introduction

Temperature optical fiber sensors are of the utmost importance in a wide range of fields such as oil and gas exploration [1] and the electrical power industry (e.g., for finding hot spots in a distribution line [2,3]), as they can offer high-performance operation in electrically and chemically harsh environments. Fiber Bragg gratings in conventional single-mode fibers have, therefore, been widely employed in research and industry, in discrete sensing systems, presenting a sensitivity of ~13 pm/°C [4].

One additional advantage of fiber sensors, unavailable for their electrical counterparts, is the possibility of offering distributed sensing over meters or even kilometers of length. For this purpose, sensors based on Raman [5] and Brillouin [6] scattering have been developed and widely studied. Raman-scattering-based temperature sensors measure the backscattered anti-Stokes to Stokes intensity ratio, which is temperature dependent. However, high signal-to-noise ratios invariably require pumping with peak powers of at least a few watts [5]. Distributed sensing along up to a few tens of kilometers and spatial resolutions of around 1 m were achieved with response times of tens of seconds [7]. More complex techniques, such as photon counting, allow resolution of 10 cm but increase the time response to up to 1 min [8].

Brillouin-scattering-based sensors rely on measuring the frequency shift provided by Brillouin scattering. The higher scattering efficiency means that lower powers are required, compared to Raman-based sensors, but the smaller spectral separation between pump and scattered light makes necessary

1559-128X/13/071461-07$15.00/0
© 2013 Optical Society of America

the use of more complex detection and processing schemes [9]. Sensing along up to 150 km with a resolution of 2 m and sensing over 2 km with a resolution of 2 cm have been achieved [10]. One issue that limits Brillouin-based temperature sensors, which also affects Bragg grating sensors, is the cross sensitivity between temperature and strain.

Similarly to fiber Bragg gratings, photonic bandgap (PBG) fibers [11] present resonant spectral features, which shift with the environmental conditions that affect the index profile of the fiber structure. Although the air-silica structure of hollow-core PBG fibers [12] is known to provide very low temperature sensitivities because of the low air thermo-optic coefficient [13], temperature sensors can, in principle, be developed in PBG fibers with higher-index axial inclusions. In these fibers, the inclusions are periodically distributed in a lower refractive index host, normally silica, thus forming the transverse 2D photonic crystal.

The use of PBG fibers for temperature sensing has been demonstrated, but the large majority of reports have focused on air-silica solid-core photonic-crystal fibers, the cladding holes of which are filled with liquid crystals or high-index liquids, to create the PBG [14–17]. Temperature sensitivities up to 27 nm/°C have been reported for temperatures up to 90°C [14]. The high sensitivity, on the other hand, limits the temperature range to tens of degrees Celsius before the bandgaps vanish. Another limitation of this approach is the impossibility of filling fibers much longer than a few centimeters, which drastically limits the development of distributed sensors.

The all-solid PBG (AS-PBG) fiber [18] is a kind of silica photonic-crystal fiber in which the higher-index inclusions are composed of doped-silica rods, so that no liquid materials are required for the formation of a temperature-sensitive PBG. As the final fiber structure is directly obtained during the drawing process, lengths of hundreds of meters to kilometers can be obtained, allowing for distributed sensing.

Temperature sensors using optical fibers with higher-index inclusions have been demonstrated in ARROW fibers [19] and AS-PBG fibers [20], but they exploit interference between core-guided modes and modes that are guided in or that extend to the first ring of rods around the core. Excitation of the desired modes is achieved by splicing a few millimeters of the fiber between conventional fibers. Sensitivities of up to 71.5 pm/°C were achieved [19], but this technique allows only for discrete measurements or, at best, quasi-distributed sensing if several sections of the bandgap fiber are used interleaved with conventional fibers. In addition, the measurable temperature range is limited by the periodicity of the spectrum resulting from interference.

In this paper, the temperature sensitivity of transmission in an AS-PBG silica fiber, with higher-index rods consisting of germanium-doped silica, is characterized, for the first time to the best of our knowledge, aiming at distributed and discrete temperature sensors. Either the bandgap spectral shift or the transmitted intensity at a fixed wavelength near the bandgap edge can be monitored. We investigate the fiber response when either a section or its entire length is heated, as well as the temperature sensitivity increase when a small fiber section is tightly bent. A semi-analytical mathematical method is used to estimate the bandgap spectral positions in a straight fiber, as well as their shift with temperature.

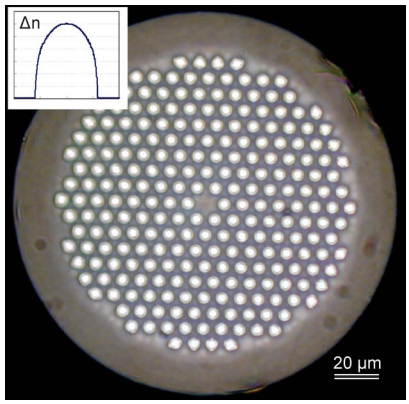

Fig. 1. (Color online) AS-PBG fiber microscopy image. Inset: radial refractive index contrast profile (in linear scale) of a high-index rod.

2. Fiber Characteristics and Transmission Spectra

The fiber used was the AS-PBG fiber shown in Fig. 1. The germanium-doped rods (lighter spots in the figure) have a diameter of 4.1 μm, an interrod spacing (pitch, Λ) of 7.4 μm, and the refractive index contrast profile, Δn, shown in the inset of Fig. 1. The peak contrast is of ~3%. The core diameter is 10.1 μm. Figure 2 shows the experimentally obtained fiber transmission (green curve), measured using a supercontinuum source and an optical spectrum analyzer

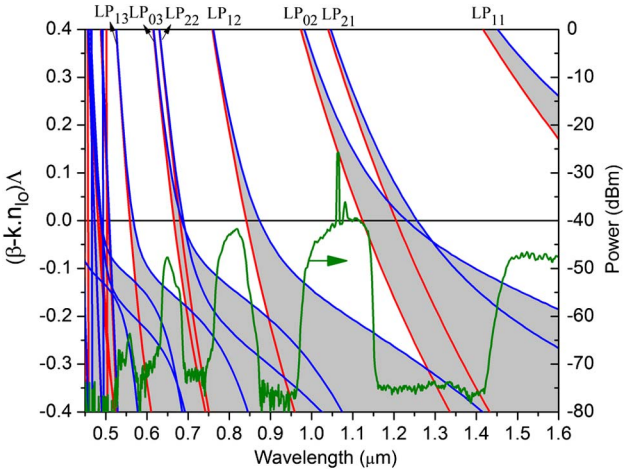

Fig. 2. (Color online) Calculated band structure in the cladding of the AS-PBG fiber (left axis) and measured fiber transmission spectrum (right axis).

(OSA). Five PBGs can be observed in the 500–1600 nm wavelength range.

The position of these bandgaps was also predicted using the semi-analytical model developed in [21], which is based on the Bloch modes calculation in one cell of the cladding photonic crystal. This method consists of computing the boundaries of the gray regions in Fig. 2, where cladding modes exist. These modes consist of a collection of supermodes formed by beyond-cutoff linearly polarized, LP_{lm} ($l = 0, 1, 2, \ldots$; $m = 1, 2, 3, \ldots$), modes of the higher-index rods. In the gaps between these regions, and for propagation constants, β, below the wavenumber of light in the lower refractive index material ($k \cdot n_{lo}$, with k being the wavenumber in vacuum and n_{lo} the refractive index of the material), there can be guided core modes. Indeed, it can be seen that good agreement is achieved between the predicted bandgap regions and the experimental high transmission spectral ranges.

For these calculations, the silica refractive index, $n_{lo} = n_{SiO_2}$, was obtained using its Sellmeier equation [22], and the refractive index of the rods, n_{hi}, was assumed to be uniform and calculated through [23]:

$$n_{hi} = x n_{GeO_2} + (1 - x) n_{SiO_2}, \quad (1)$$

where n_{GeO_2} is the refractive index of germania, calculated via its Sellmeier equation [24], and x is the germania molar fraction, assumed to be 0.32, as it gives the known refractive index contrast of ~3% for this fiber. For simplicity, a step refractive index profile is assumed, which allows for band calculation through the model developed in [21]. The good agreement with the experimental measurement, shown in Fig. 2, indicates the suitability of this approximation.

As previously described in [25], it was experimentally observed that, due to the relatively low refractive index contrast, the bandgaps present a high sensitivity to fiber bending. The transmission spectrum within two bandgaps is shown in Fig. 3 for various bend radii (and for a single-turn coil). Consistent with [25], it is possible to note the narrowing of the bandgaps, which is more apparent in the blue edges (shorter wavelengths). As shown in Section 3, bending also affects the transmission spectrum temperature dependence, which can be exploited for the development of discrete and reconfigurable sensors.

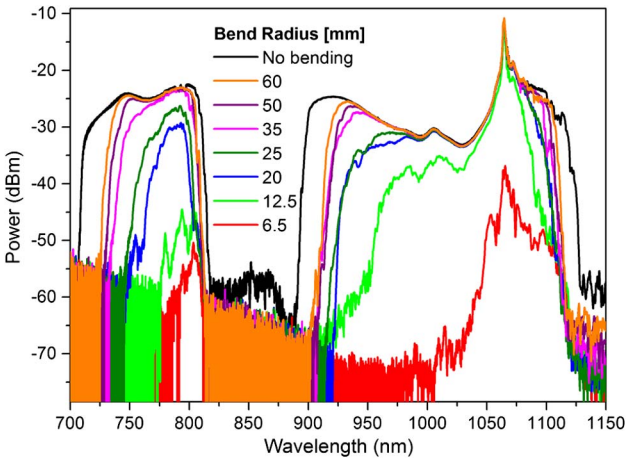

Fig. 3. (Color online) AS-PBG fiber transmission spectrum for different single-turn coil radii (total fiber length fixed at 40 cm).

3. Sensitivity to Temperature

The AS-PBG fiber temperature-dependent bandgap spectral shift was characterized under three different conditions, shown in Fig. 4. In all cases, a broadband source was used and the transmitted spectra were measured in an OSA. The first set of experiments, shown in Fig. 4A, was undertaken using 25 and 50 cm lengths of AS-PBG fiber spliced between conventional index guiding fibers. The whole length of the AS-PBG fiber was heated. In addition to discrete temperature sensing, this scheme may be exploited for quasi-distributed wavelength-multiplexed sensing geometries, by interleaving several AS-PBG fiber sections, with similar bandgaps but different bandgap edge spectral positions, with conventional fibers. The second set of experiments, shown in Fig. 4B, consisted of heating a 2 m section of a 10 m long AS-PBG fiber, which emulated the situation of a fully distributed sensor. Finally the third group of experiments, Fig. 4C, was made by bending a short (few centimeters) section of the AS-PBG fiber to a tight bend radius, which locally increased its sensitivity to temperature. This configuration can be exploited for discrete sensing, with the unusual characteristic that the position of the sensor can easily be reconfigured over a long length of fiber by simply changing the position where bending is induced.

A. Setup A: All the Fiber Length Heated

For the first set of experiments, a supercontinuum source was used that consisted of a commercial photonic-crystal fiber (NL-1040 from crystal fibre) pumped by a subnanosecond pulsed laser at

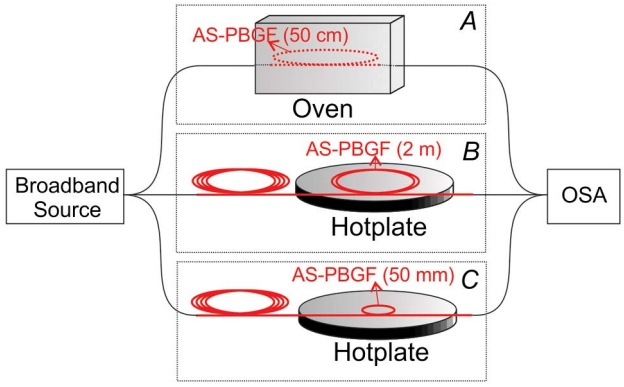

Fig. 4. (Color online) Experimental setups used to characterize the temperature sensitivity of the AS-PBG fiber. In case (A), the whole fiber length is heated inside an oven, in (B) a 2 m section of a 10 m long fiber is heated on a hotplate, and in (C) a 50 mm section of a 10 m long fiber is heated under a tight bend.

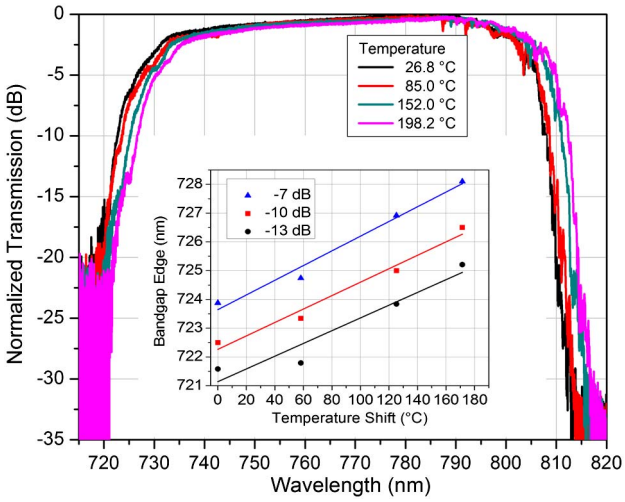

Fig. 5. (Color online) Fiber normalized transmission spectrum for different temperatures when the full length (50 cm) of an AS-PBG fiber is heated. Inset: bandgap edge position at fixed transmission levels (indicated in the legend) as temperature function and linear fitting curves.

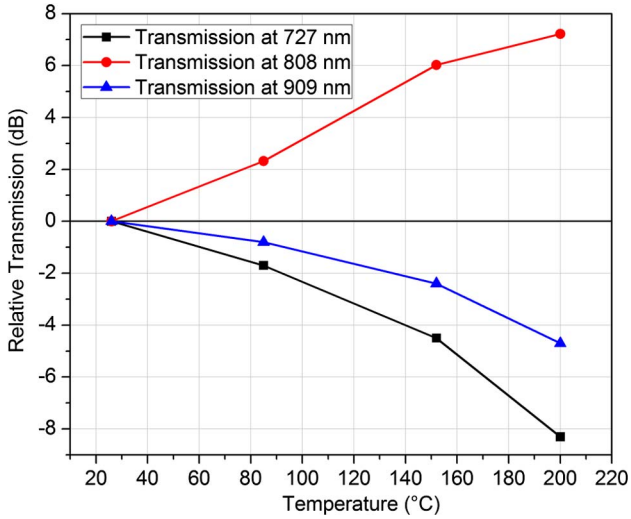

Fig. 6. (Color online) Transmission power variation at fixed wavelengths as a function of temperature.

1064 nm. The NL-1040 fiber was spliced to a single-mode fiber (cutoff wavelength at ~600 nm), which in turn was spliced to the AS-PBG fiber that was spliced at the output tip to another single-mode fiber. The entire AS-PBG fiber length was heated in an oven and the transmitted light was then measured in an OSA, as shown in Fig. 4A. The normalized transmission spectrum for a 50 cm length fiber (coiled with a 90 mm radius) for different temperatures is shown in Fig. 5. Temperature affects the fiber mainly via the thermo-optic effect, which increases the material refractive index and, consequently, the optical path for the propagating light. As a result, a bandgap shift toward longer wavelengths is observed when the fiber is heated. The inset in Fig. 5 shows the blue (shorter wavelength) bandgap edge spectral position measured by tracking the point at which transmission is at −7, −10, and −13 dB from its maximum. For the −10 dB case, the linear fit gives a sensitivity of 23.4 pm/°C with a standard error of 2.5 pm/°C. Measurements taken at −7 dB from the maximum transmission yield a similar sensitivity of 25.5 pm/°C with the same standard error, while measurements at the −13 dB level, a noisier level, gives a sensitivity of 22.2 pm/°C and an error of 4.5 pm/°C. These results have shown to be reproducible. As these sensitivity values agree to one another within the measurement errors, we conclude that, within the investigated 6 dB transmission level range, the exact choice of the level minimally affects the results.

Alternatively, to quantify the temperature sensitivity, it is possible analyze the power transmission at a fixed wavelength near the bandgap edges. Since these edges are steep, this approach allows for high-sensitivity intensity-encoded sensors to be obtained. Figure 6 shows the variation in transmitted power, relative to the room temperature value, for three fixed wavelengths near the bandgap edges. A ~7.2 dB transmission increase is obtained at 808 nm for a temperature variation of 175°C. The positive variation in transmission is expected, as this wavelength lies in the red edge of the transmission band shown in Fig. 5. On the other hand, a negative transmission variation (of 8.3 dB over the same 175°C temperature range) is observed at 727 nm, also shown in Fig. 6, because this point is located near the blue edge of the transmission window. Temperature sensing simultaneously using two wavelengths in opposite bandgap edges may distinguish temperature effects from effects such as undesired optical loss variations and AS-PBG fiber bends, since these effects will cause power variations of same sign (see Fig. 3 for the bend loss case), while temperature will lead to power increase at one wavelength and to power decrease at the other. The transmission variation at 909 nm, located near the blue edge of another fiber bandgap (which presents a similar temperature-dependent spectral shift of ~23 pm/°C), not shown in Fig. 5, is also depicted in Fig. 6.

Although the fiber in these experiments was coiled with a large curvature radius, in order to compare the resulting bandgap shift with that predicted by a simple mathematical model that does not account for bending, the experiment was repeated with a 25 cm length of fiber, which was kept straight while heated. The spectral shift for the bandgap that extends from ~900 to 1135 nm, measured by tracking the −10 dB normalized transmission point, can be seen in Fig. 7. For that case, the sensitivity for the red bandgap edge is 35 pm/°C with a standard error of 3 pm/°C, while the sensitivity in the blue edge is 19 pm/°C with an error of 1.2 pm/°C.

The mathematical model used in Section 2 to calculate the bandgap edges was then altered to account for, in Eq. (1), the thermo-optic coefficients

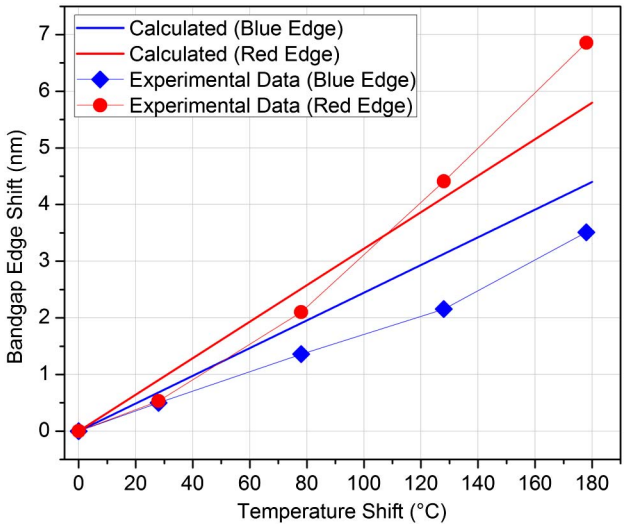

Fig. 7. (Color online) Calculated (solid line) and measured (diamonds and circles) spectral shifts with temperature in the 900–1135 nm bandgap.

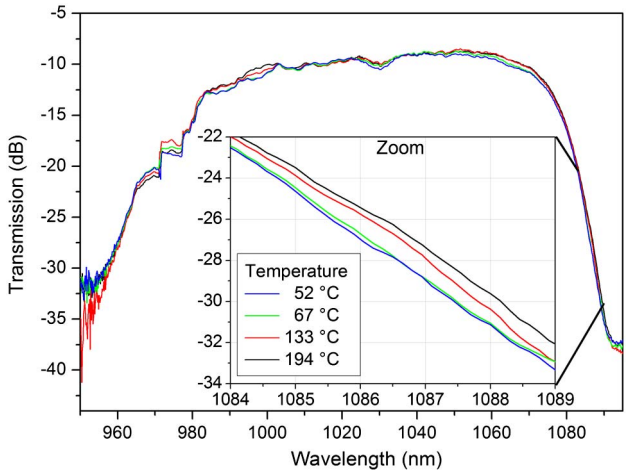

Fig. 8. (Color online) Transmission spectra for different temperatures when a 2 m section of a 10 m AS-PBG fiber is heated.

of both silica, $dn/dT = 11 \times 10^{-6}°C^{-1}$ [26], and germania, $dn/dT = 18 \times 10^{-6}°C^{-1}$ [27]. Silica's thermal expansion coefficient, $0.55 \times 10^{-6}°C^{-1}$ [4], was also assumed for the whole fiber structure. Possible structural stresses due to different expansion coefficients between the doped rods and the silica background were neglected. Figure 7 also shows the calculated band structure shift with temperature (solid lines). The good qualitative match between the results allow one to conclude that the thermo-optic effect is, indeed, the dominant effect, and that the increase in the refractive index contrast due to the higher thermo-optic coefficient of germania leads to a bandgap broadening, with a larger shift observed in the red bandgap edge.

B. Setup B: Long-Length Fiber Section Heated

The second set of measurements, as shown in Fig. 4B, is aimed at characterizing the AS-PBF fiber spectral response when only a fraction of the fiber length is heated. Although demonstrating spatially resolved temperature sensitivity is beyond the scope of this paper, the fiber characterization under these conditions is the first step toward a distributed temperature sensor based on an AS-PBG fiber. In this case, the amplified spontaneous emission from an ytterbium-doper fiber was used as a broadband source. This fiber was pumped with a 980 nm cw diode laser and was spliced to a ~10 m length AS-PBG fiber. A ~2 m long section of the latter fiber was coiled, with a bend radius of ~60 mm, over a hotplate and heated.

The bandgap transmission for different temperatures is shown in Fig. 8. The bandgap shift, if the point in the red edge with −24 dB transmission is tracked as temperature is increased, is of ~1 nm for a temperature variation of 142°C, giving an average sensitivity of ~7 pm/°C. If the transmission at a fixed wavelength in the bandgap edge, in this case 1086 nm, is monitored, a 1.6 dB transmission variation (increase) is observed for the 142°C temperature change. The reduced temperature sensitivity of the spectrum, compared with the measurements in which the entire fiber was heated, can be seen as the effect of the concatenation of the transmission in the heated and unheated sections. The use of reflectometry techniques would then provide distributed temperature information with sensitivities comparable those in the previous set of experiments. For this purpose, the use of an appropriate AS-PBG fiber is necessary, in which the reflectometer probe wavelength lies in one of the bandgap edges.

Note that in addition to the transmission-edge shift, the inset of Fig. 8 shows that the edge profile slightly varies with temperature. This feature may be attributed to the fact that the heated fiber section is subjected to temperature gradients, which increase with temperature, due to nonuniform heating across the hotplate surface. This spectral feature, thus, appears to be further evidence that distributed sensing is viable.

C. Setup C: Short-Length Bent Fiber Section Heated

The last set of experiments, Fig. 4C, explores bending effects on the bandgap transmission and, as found by our measurements, the increase in temperature sensitivity provided by bending. A 50 mm section of the 10 m AS-PBG fiber was coiled into a loop with an 8 mm radius and heated. Figure 9 shows the obtained transmission spectra as a function of temperature. As in Fig. 3, the narrower spectra are attributed to the bent fiber region; therefore, any spectral shift in transmission is primarily attributed to the coiled section. It is seen that, taking the −21 dB transmission level as a reference (and considering a ±1 dB error in determining this level), spectral shifts of 8.8 ± 2.0 nm in the blue bandgap edge and 2.9 ± 0.1 nm in the red edge are observed over the tested temperature range of 207°C, which yields average temperature sensitivities of

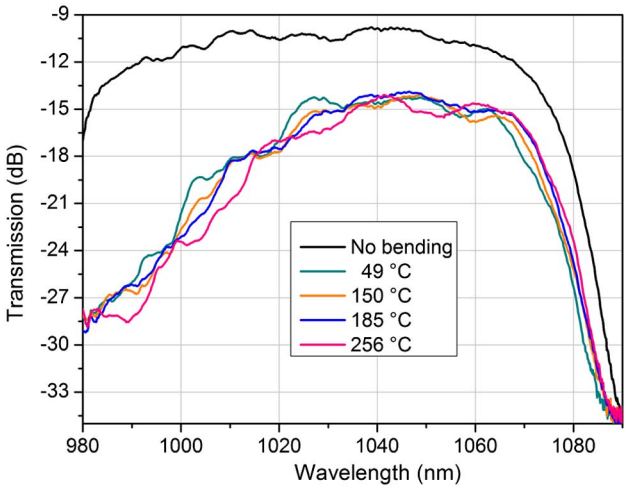

Fig. 9. (Color online) Fiber transmission for different temperatures when a single-turn coil with a 8 mm radius is heated.

$\sim 42.5 \pm 9.7$ pm/°C and $\sim 14 \pm 0.5$ pm/°C, respectively. These shifts are higher then those obtained in the previous set of experiments (second set of experiments), with a much shorter fiber length, especially in the blue bandgap edge. A discrete temperature sensor can, therefore, be envisaged, in which sensitivity is primarily obtained in the bent section of a longer fiber. The sensor position can easily be changed by simply changing the position where the fiber is bent.

Figure 9 also shows that the blue bandgap edge of the bent fiber is spectrally noisier (although temporally stable), which results in a nonlinear bandgap shift with temperature. The red edge, on the other hand, presents a linear shift of ~14 pm/°C, comparable to that obtained in fiber Bragg gratings at 1550 nm [4]. For fixed-wavelength transmission measurements, a 1.4 dB transmission increase is obtained at 1080 nm and a ~2 dB transmission decrease is achieved at 1005 nm over a 140°C temperature variation. These transmission variations are comparable to those obtained in the previous set of experiments, despite the fact that the heated fiber length corresponds to a two orders of magnitude lower fraction of the total fiber length. This feature corroborates the improved temperature sensitivity of bent fiber sections, even though a slight reduction in the bandgap edge steepness is observed in the spectrum due to bending.

4. Conclusions

The spectral response to temperature of an AS-PBG was investigated for the first time to our knowledge. In addition, such a fiber was considered as a sensor under three different conditions that aim at distributed, quasi-distributed, and discrete sensing. The results show that this fiber can be used as a temperature sensor for at least up to a few hundreds of degrees Celsius. The sensing scheme is based upon the PBG shift, which, as a developed theoretical model shows, occurs mainly due to the thermo-optic coefficients of silica and doped-silica high-index inclusions. Sensitivities of up to ~35 pm/°C were achieved when a fiber of 25 cm length was heated in all its extension, which is suitable for discrete or quasi-distributed sensing. Bent fiber sections are shown to improve the temperature sensitivity, presenting similar temperature responses for one-order-of-magnitude shorter sections, which can be exploited in novel reconfigurable discrete sensors. The possibility to reconfigure the position of the sensing head during operation is not available in most fiber sensors, and is a major asset of the described fiber. Finally, heating a 2 m long section of a longer fiber resulted in a temperature sensitivity of ~7 pm/°C. Distributed sensing may, thus, be developed using reflectometry techniques, provided that a fiber is available with a bandgap edge at the operating wavelength of a reflectometer.

This work was partially funded by CNPq, Mackpesquisa, and FINEP.

References

1. H. Nakstad and J. T. Kringlebotn, "Oil and gas applications probing oil fields," Nat. Photonics **2**, 147–149 (2008).
2. R. Willsch, W. Ecke, and H. Bartelt, "Optical fiber grating sensor networks and their application in electric power facilities, aerospace and geotechnical engineering," in *Optical Fiber Sensors Conference Technical Digest* (IEEE, 2002), pp. 49–54.
3. P. E. Sanders, "Fiber-optic sensors: playing both sides of the energy equation," Opt. Photonics News **22**(1), 36–42 (2011).
4. A. Othonos, "Fiber Bragg gratings," Rev. Sci. Instrum. **68**, 4309–4341 (1997).
5. J. P. Dakin, D. J. Pratt, G. W. Bibby, and J. N. Ross, "Distributed optical fibre Raman temperature sensor using a semiconductor light source and detector," Electron. Lett. **21**, 569–570 (1985).
6. X. Bao, J. Dhliwayo, N. Heron, D. J. Webb, and D. A. Jackson, "Experimental and theoretical studies on a distributed temperature sensor based on Brillouin scattering," J. Lightwave Technol. **13**, 1340–1348 (1995).
7. R. Bernini, A. Minardo, and L. Zeni, "Distributed optical fiber sensors," in *An Introduction to Optoelectronic Sensors*, Vol. **7** of Series in Optics and Photonics (World Scientific Publishing Company, 2009), pp. 77–94.
8. R. Feced, M. Farhadiroushan, V. A. Handerek, and A. J. Rogers, "A high spatial resolution distributed optical fiber sensor for high-temperature measurements," Rev. Sci. Instrum. **68**, 3772–3776 (1997).
9. M. A. Soto, G. Bolognini, and F. D. Pasquale, "Analysis of optical pulse coding in spontaneous Brillouin-based distributed temperature sensors," Opt. Express **16**, 19097–19111 (2008).
10. X. Bao and L. Chen, "Recent progress in Brillouin scattering based fiber sensors," Sensors **11**, 4152–4187 (2011).
11. P. Russell, "Photonic-crystal fibers," J. Lightwave Technol. **24**, 4729–4749 (2006).
12. J. C. Knight, J. Broeng, T. A. Birks, and P. Russell, "Photonic bandgap guidance in optical fibers," Science **282**, 1476–1478 (1998).
13. Q. Shi, F. Lv, Z. Whang, L. Jin, J. J. Hu, Z. Liu, G. Kai, and X. Dong, "Environmentally stable Fabry–Pérot-type strain sensor based on hollow-core photonic bandgap fiber," IEEE Photon. Technol. Lett. **20**, 237–239 (2008).
14. T. T. Alkeskjold, J. Lægsgaard, A. Bjarklev, D. S. Hermann, J. Broeng, J. Li, S. Gauza, and S.-T. Wu, "Highly tunable large-core single-mode liquid-crystal photonic bandgap fiber," Appl. Opt. **45**, 2261–2264 (2006).
15. T. R. Wolinski, A. Czapla, S. Ertman, M. Tefelska, A. W. Domanski, J. Wojcik, E. Nowinowski-Kruszelnicki, and

R. Dabrowski, "Photonic liquid crystal fibers for sensing applications," IEEE Trans. Instrum. Meas. **57**, 1796–1802 (2008).
16. L. Scolari, S. Gauza, H. Xianyu, L. Zhai, L. Eskildsen, T. T. Alkeskjold, S.-T. Wu, and A. Bjarklev, "Frequency tunability of solid-core photonic crystal fibers filled with nanoparticle-doped liquid crystals," Opt. Express **17**, 3754–3764 (2009).
17. N. M. Litchnitser and E. Poliakov, "Antiresonant guiding microstructured optical fibers for sensing applications," Appl. Phys. B **81**, 347–351 (2005).
18. F. Luan, A. K. George, T. D. Hedley, G. J. Pearce, D. M. Bird, J. C. Knight, and P. St. J. Russell, "All-solid photonic bandgap fiber," Opt. Lett. **29**, 2369–2371 (2004).
19. S. H. Aref, O. Frazão, L. A. Ferreira, F. M. Araújo, J. L. Santos, H. Latifi, P. Foy, T. Hawkins, J. Ballato, T. Her, and F. Farahi, "Modal interferometer based on ARROW fiber for strain and temperature measurement," IEEE Photon. Technol. Lett. **21**, 1636–1638 (2009).
20. Y. Geng, X. Li, X. Tan, Y. Deng, and Y. Yu, "Mode-beating-enabled stopband narrowing in all-solid photonic bandgap fiber and sensing applications," Opt. Express **19**, 8167–8172 (2011).
21. T. A. Birks, G. J. Pearce, and D. M. Bird, "Approximate band structure calculation for photonic bandgap fibres," Opt. Express **14**, 9483–9490 (2006).
22. G. Ghosh, M. Endo, and T. Iwasaki, "Temperature-dependent Sellmeier coefficients and chromatic dispersions for some optical fiber glasses," J. Lightwave Technol. **12**, 1338–1342 (1994).
23. A. S. Huang, Y. Arie, C. C. Neil, and J. M. Hammer, "Study of refractive index of GeO2:SiO2 mixtures using deposited-thin-film optical waveguides," Appl. Opt. **24**, 4404–4407 (1985).
24. M. Bass, *Handbook of Optics Volume II Devices, Measurements and Properties*, 2nd ed. (McGraw-Hill, 1995).
25. A. Argyros, T. A. Birks, S. G. Leon-Saval, C. M. B. Cordeiro, and P. St. J. Russell, "Guidance properties of low-contrast photonic bandgap fibres," Opt. Express **13**, 2503–2511 (2005).
26. G. Ghosh, "Model for the thermo-optic coefficients of some standard optical glasses," J. Non-Cryst. Solids **189**, 191–196 (1995).
27. T. Mizunami, T. Fukuda, and A. Hayash, "Fabrication and characterization of long-period-grating temperature sensors using Ge-B-codoped photosensitive fibre and single-mode fibre," Meas. Sci. Technol. **15**, 1467–1473 (2004).